2D3-5

Target Response Extraction from Measured GPR Data

#Masahiko Nishimoto, Daisuke Yoshida, Kohichi Ogata, and Masayuki Tanabe
Graduate School of Science and Technology, Kumamoto University
2-39-1 Kurokami, Kumamoto 860-8555, Japan, nisimoto@cs.kumamoto-u.ac.j

1. Introduction

Ground penetrating radar (GPR) is one of the most useful sensors for detection and identification of shallowly buried objects such as anti-personnel landmines in the ground [1]. However, for practical application of GPR systems to detect and identify shallowly buried objects, it is still insufficient for accurate detection and identification because of strong ground clutter. In order to use GPR systems successfully for target detection and identification, it is necessary to extract the target response accurately from measured GPR data. As an incident pulse, a simple shape waveform such as a monocycle pulse with a sharp peak and narrow width is convenient for time-domain analysis [2]. In actual measurement situation, however, the pulse waveform is distorted by characteristics of transmitting and receiving antennas when the pulse is radiated and received by the antenna pair. Therefore, a calibration that eliminates the antenna characteristics and makes the desired pulse waveform is important for accurate detection and identification. In our previous study [3][4], we proposed a method for calibration of the pulse waveform using a metal plate reflection as a reference data, and applied it to measured responses from objects in free space. In this study, we apply the method to responses from buried objects and demonstrate that the calibration of GPR responses is significant for reliable target response extraction [5].

2. Inverse Filter for Waveform Calibration

For convenience, we shall briefly summarize the procedure of waveform calibration described in the References [3] and [4]. Figure 1 shows monostatic radar signal measurement using a GPR system considered in this study. Target responses from the buried object in shallow depth are measured together with the strong ground clutter and crosstalk between the transmitting and receiving antennas. This measurement can be expressed in terms of transfer functions, as illustrated in Fig. 2. Thus, the received signal in frequency domain can be expressed as

$$\begin{aligned} G(\omega) &= H_{Rx}(\omega)H_{ptf}(\omega)H_{targ}(\omega)H_{ptb}(\omega)H_{Tx}(\omega)\cdot F(\omega) \\ &\quad + H_{Rx}(\omega)H_{psf}(\omega)H_{surf}(\omega)H_{psb}(\omega)H_{Tx}(\omega)\cdot F(\omega) + H_{Rx}(\omega)H_{crs}(\omega)H_{Tx}(\omega)\cdot F(\omega) \end{aligned} \quad (1)$$

where H_{Tx} and H_{Rx} are transfer functions of transmitting and receiving antennas, H_{targ} and H_{surf} are transfer functions of scattering by the target and ground surface, H_{ptf}, H_{ptb}, H_{psb}, and H_{psb} are transfer functions of propagation paths between antennas and the target or ground surface, H_{crs} represents antenna crosstalk, and $F(\omega)$ and $G(\omega)$ are spectra of incident and received pulses, respectively. The first term on the right hand side of Eq. (1) is a target response, the second is a ground clutter, and the third is a crosstalk between the transmitting and receiving antennas. Measurements of the target response with a vector network analyzer allow us to measure the S parameter, and the S parameter of target response S_{targ} corresponding to Eq. (1) is expressed as follows:

$$S_{targ} = H_{ANT}(\omega)H_{ptt}(\omega)H_{targ}(\omega) + H_{ANT}(\omega)H_{pst}(\omega)H_{surf}(\omega) + H_{ANT}(\omega)H_{crs}(\omega) \quad (2)$$

where $H_{ANT}(\equiv H_{Tx}\cdot H_{Rx})$ is the total antenna characteristics to be eliminated, $H_{ptt}(\equiv H_{ptf}\cdot H_{ptb})$ and $H_{pst}(\equiv H_{psf}\cdot H_{psb})$ are transfer functions that correspond to propagation. Since the second term

of the above equation is antenna crosstalk, it can easily be determined from the measured response when there is no target. After subtracting the antenna crosstalk, we have the following expression:

$$S_{targ} - S_{free} = H_{ANT}(\omega) H_{ptt}(\omega) H_{targ}(\omega) + H_{ANT}(\omega) H_{pst}(\omega) H_{surf}(\omega) \tag{3}$$

Next, in order to remove the effect of the antenna characteristics H_{ANT} that causes undesirable waveform distortion, we now design an inverse filter that can eliminate the antenna characteristics. As a reference data for waveform calibration, we introduce S parameter $\overline{S}_{surf}$ that corresponds to a reflection from a flat ground surface. This can be obtained from a simple additional measurement and is expressed as

$$\overline{S}_{surf} - S_{free} = H_{ANT}(\omega) \overline{H}_{pst}(\omega) \overline{H}_{surf}(\omega) \tag{4}$$

where $\overline{H}_{surf}$ is the complex scattering amplitude of the response from the flat ground surface and $\overline{H}_{pst}$ is the transfer function for the path between two antennas and the ground surface. Using this equation, the inverse filter can be expressed as follows:

$$H_{ANT}^{-1}(\omega) = \frac{1}{\overline{S}_{surf} - S_{free}} \overline{H}_{pst}(\omega) \overline{H}_{surf}(\omega) \tag{5}$$

Taking account of the facts that the complex scattering amplitude $\overline{H}_{surf}$ corresponds to Fresnel reflection coefficient and can be approximated to be constant, we have

$$\overline{H}_{surf}(\omega) \approx R \text{ (constant)}, \quad \overline{H}_{pst}(\omega) \approx \frac{1}{r^2} e^{-j\omega t_0} \tag{6}$$

where r is a distance between antenna aperture and ground surface, and t_0 corresponds to the delay time needed for the pulse to travel back and forth between the antennas and the ground surface. Thus, we can obtain the following simple expression:

$$H_{ANT}^{-1}(\omega) = -\frac{A}{\overline{S}_{surf} - S_{free}} e^{-j\omega t_0} \tag{7}$$

where A is a positive constant inversely proportional to the square of the distance r. By applying this inverse filter to measured GPR response expressed Eq. (3), we can eliminate the effect of the antenna characteristics as follows:

$$H_{ptt}(\omega) H_{targ}(\omega) + H_{pts}(\omega) H_{surf}(\omega) = -\left(\frac{S_{targ} - S_{surf}}{\overline{S}_{surf} - S_{free}} \right) \exp(-j\omega t_0) \tag{8}$$

Since the coefficient A is related only to the amplitude of the target response, it was set to $A = 1$. The first and the second terms in the left hand side correspond to the scattering transfer function of target response and ground clutter, respectively. Thus, we can obtain time-domain responses for desired incident waveforms. The response $g(t)$ from the target under the incident pulse f(t) can be calculated by the inverse Fourier transformation as follows:

$$\begin{aligned} g(t) &= g_{targ}(t) + g_{surf}(t) \\ &= \frac{1}{2\pi} \int_{-\infty}^{\infty} H_{ptt}(\omega) H_{targ}(\omega) F(\omega) \exp(j\omega t) d\omega + \frac{1}{2\pi} \int_{-\infty}^{\infty} H_{pst}(\omega) H_{surf} F(\omega) \exp(j\omega t) d\omega \\ &= -\frac{1}{2\pi} \int_{-\infty}^{\infty} \left(S_{targ} - S_{surf}\right) / \left(\overline{S}_{surfl} - S_{free}\right) F(\omega) \exp[j\omega (t - t_0)] d\omega \end{aligned} \tag{9}$$

Although the response $g(t)$ is not distorted by the antenna characteristics, it still includes the ground clutter $g_{surf}(t)$. However, the ground clutter can easily be subtracted because the ground clutter and the target response are separated each other in time-domain after the calibration.

3. Evaluation of Calibration Using Experimental Data

In order to evaluate the waveform calibration mentioned above, we apply it to measured data obtained by a laboratory experiment. Figure 3 shows the UWB-GPR antennas used for our measurements [4]. The identically shaped Tx and Rx Vivaldi antennas are in a metal box (shield case) with one open end in order to suppress radiation to the sides and back, and the inner wall of the shield case is loaded with electromagnetic wave absorber to reduce internal resonance that causes strong antenna ringing. This antenna set is usable from 1 GHz to 6 GHz, which is the intended band for our experiment. Figure 4 shows schematic drawing of the experiment. As the incident pulse with simple waveform, we employ a monocycle pulse as shown in Fig. 5.

Figure 6 shows measured raw and calibrated pulse responses from a plastic dummy of Type-72 anti-personnel landmine [4]. The depth of the dummy is 5.0 cm from the ground surface. In Fig. 6(a), we can see that the measured waveform has the late-time response caused by the resonance inside the shield case and the desired target response is completely hidden in the part. After applying the calibration procedure, as shown in Fig. 6(b), the late-time response is suppressed and the target response appears clearly. From this result, we can get the confirmation that the waveform calibration applied here provides a good result and is significant for target response extraction.

4. Conclusions

In this study, we have applied the method for waveform calibration to GPR responses from buried objects and have demonstrated that the calibration of GPR responses is essential procedure and is significant for reliable target identification.

References

[1] D. J. Daniels (Ed.), "*Ground Penetrating Radar (2nd Edition)*," Institution of Engineering and Technology (IET) Radar, Sonar, Navigation and Avionics Series 15, IET, 2004.

[2] M. Nishimoto, K. Nagayoshi, S, Ueno, and Y. Kimura, "Classification of landmine-like objects buried under rough ground surface using a ground penetrating radar," *IEICE Trans. Electron.*, vol. E90-C, no. 2, pp.327-333, February, 2007.

[3] M. Nishimoto and K. Tomura, "Inverse Filtering Operation for Reconstruction of Distorted GPR Response", *Proceedings of the TENCON 2010*, November, 2011.

[4] M. Nishimoto, K. Tomura, and K. Ogata, "Waveform calibration of ground penetrating radars for identification of buried objects", *IEICE Trans. Electron.*, vol. E95-C, pp.105-109, 2012.

[5] M. Nishimoto, D. Yoshida, K. Ogata, and M. Tanabe, "Extraction of Target Response from GPR data for Identification of Buried Objects", *submitted to IEICE Trans. Electron.,2012*

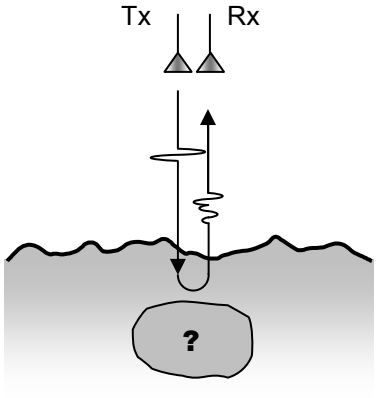

Fig.1. Measurement of radar response from a shallowly buried object using GPR.

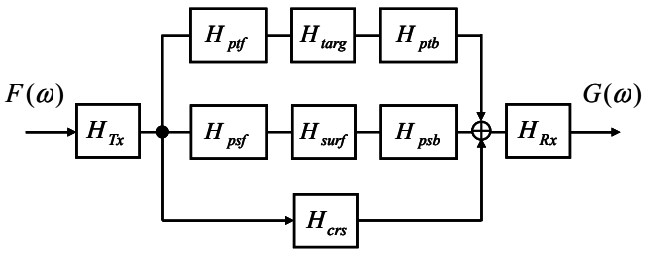

Fig. 2. Block diagram of measurement expressed in terms of the transfer functions.

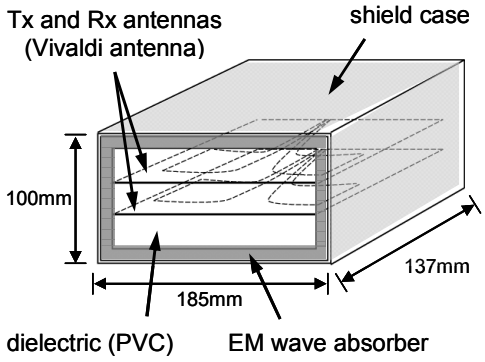

Fig. 3. GPR antenna set with a shield case used for the measurement [4].

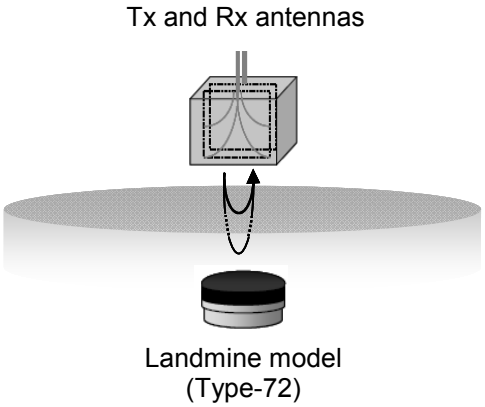

Fig. 4. Schematic drawing of the experiment. (Depth of the landmine: 5 cm)

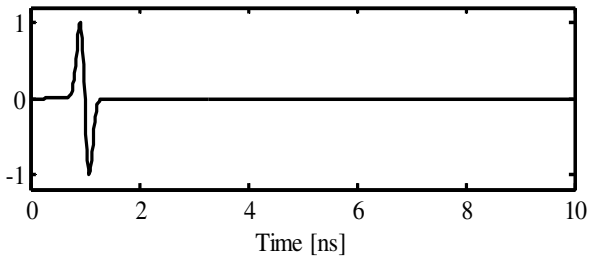

Fig. 5. Incident monocycle pulse used for the experiment. (Once-differentiated Gaussian pulse)

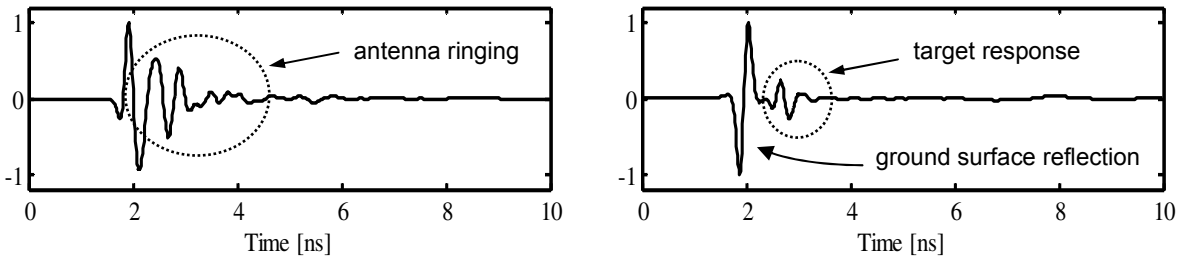

(a) Measured pulse response. (b) Pulse response after calibration.

Fig. 6. Waveform of the monocycle pulse response from the buried landmine model. (a) Measured pulse response (raw data), (b) Calibrated pulse response.